HHS Public Access

Author manuscript

J Thromb Haemost. Author manuscript; available in PMC 2019 February 01.

Published in final edited form as:

J Thromb Haemost. 2018 February ; 16(2): 316–329. doi:10.1111/jth.13907.

Hemodynamic force triggers rapid NETosis within sterile thrombotic occlusions

X. Yu[*], **J. Tan**[*], and **S. L. Diamond**[*,†]

[*]Institute for Medicine and Engineering, Department of Chemical and Biomolecular Engineering, 1024 Vagelos Research Laboratory, University of Pennsylvania, Philadelphia, PA 19104

Summary

Background—Neutrophil extracellular traps (NETs) are released when neutrophils encounter infectious pathogens, especially during sepsis. Additionally, NETosis occurs during venous and arterial thrombosis, disseminated intravascular coagulation, and trauma.

Objective—We tested if hemodynamic forces trigger NETosis during sterile thrombosis.

Methods—NETs were imaged with Sytox-green during microfluidic perfusion of Factor XIIa-inhibited or thrombin-inhibited human whole blood over fibrillar collagen (± tissue factor).

Results—For perfusions at initial inlet venous or arterial wall shear rates (100 or 1000 s^{-1}), platelets rapidly accumulated and occluded microchannels with subsequent neutrophil infiltration at either flow condition, however NETosis was detected only at the arterial condition. Shear-induced NETs (SINs) at 30 min were >150-fold greater at arterial conditions in the absence of thrombin and >80-fold greater in the presence of thrombin, relative to the venous condition. With or without thrombin, venous perfusion for 15 min generated no NETs, but an abrupt shift-up to arterial perfusion triggered NETosis within 2 min, eventually reaching levels 15 min later that were 60-fold greater than microchannels without perfusion shift-up. SINs contained citrullinated histone H3 and myeloperoxidase and were DNase-sensitive, but were not blocked by inhibitors of platelet-neutrophil adhesion, HMGB1-RAGE interaction, cyclooxygenase, ATP/ADP or PAD-4. For measured pressure gradients exceeding 70 mmHg/mm-clot across NET-generating occlusions to drive interstitial flow, calculated fluid shear stress on neutrophils exceeded the known lytic value of 150 dyne/cm^2.

Conclusions—High interstitial hemodynamic forces can drive physically entrapped neutrophils to rapidly release NETs during sterile occlusive thrombosis.

[†]Corresponding author. Tel. 215-573-5702, sld@seas.upenn.edu.

Addendum

Contribution: X. Yu, J. Tan, and S. L. Diamond designed research, wrote the manuscript, analyzed and interpreted the data; X. Yu performed the experiments; J. Tan performed the simulations.

Disclosure of Conflict of Interests

The authors declare no conflict of interests.

Supporting Information

Additional Supporting Information may be found in the online version of this article:

Keywords

Extracellular Traps; hemodynamics; histone; neutrophil; thrombosis

Introduction

Activated neutrophils can release their DNA when triggered by endotoxin or cytokines [1], pathogenic microorganisms [2], platelet-derived high-mobility group protein box 1 (HMGB1) [3,4], and autoantibodies [5]. Neutrophil extracellular traps (NETs) have antimicrobial activity [1] and provide components for contact activation of the coagulation pathway [6–8] and for tissue factor pathway inhibitor (TFPI) degradation [9]. However, NETs can also contribute to tissue damage [10]. NETs have been implicated in the pathogenesis of sepsis [11], venous thrombosis [4,12], arterial thrombosis [3,13], disseminated intravascular coagulation (DIC) [14], trauma [15,16], transfusion related acute lung injury (TRALI) [17], and autoimmune vasculitis [5].

During thrombotic or hemostatic events, sterile blood clotting is typically dominated initially by platelet accumulation with neutrophils becoming localized at later stages [18]. Display of endothelial or platelet P-selectin facilitates PSGL-1-dependent neutrophil adhesion at venous flow conditions [19]. Platelet activation by thrombin, ADP, and collagen can also induce NETs, through HMGB1 release [3]. The platelet-derived disulfide-HMBG1 drives NETosis by activating neutrophil receptor for advanced glycation end products (RAGE), a pathway present in the partial stenosis model of deep vein thrombosis (DVT) in mouse [4]. HMGB1 and NETs have also been detected in thrombi following acute myocardial infarction [13]. High dose lipopolysaccharide (LPS, 5 μg/mL) or septic plasma can activate platelet toll-like receptor 4 (TLR4) which can then drive NETosis with bacteriostatic activity [11].

Critical events during NETosis include disruption of the nuclear membrane and chromatin decondensation, followed by rupture of the plasma membrane [20]. Often, NETosis utilizes reactive oxygen species (ROS) and/or peptidylarginine deiminase 4 (PAD4) for chromatin decondensation via formation of citrullinated histones [21–23]. The extracellular decoration of neutrophil released DNA with elastase, myeloperoxidase, and citrullinated histone are key diagnostic features of NETosis [20]. NET formation has been studied in the presence of flow using endotoxin stimulation or phorbol ester stimulation [24,25]. However, the distinct role of pathophysiological hemodynamic force as a trigger or cofactor for NETosis has not been resolved.

We hypothesized that hemodynamic shearing forces may play a role in NET formation during thrombosis. Using microfluidics, the function of whole blood over collagen surfaces can be studied under conditions that either prevent or promote thrombin formation and fibrin deposition. As a clot grows under flow, fluid shear stress increases on the outer surface of the clot exposed to flow. When clotting progresses toward full occlusion, however, the reduction of luminal cross-sectional area eventually generates a significant pressure drop to reduce flow and wall shear stress, up to the point of full occlusion [26,27]. At full occlusion, the clot must withstand a pressure drop across its length (ΔP/L) and this pressure drop drives

an interstitial Darcy's flow of plasma and blood constituents through the pore space of the clot, generating interstitial stresses. Intrathrombic hemodynamic force was a potent trigger of NETosis in sterile occlusive thrombi.

Methods

Materials

All reagents were obtained as described in the Supplement.

Blood collection and Preparation

Whole blood (WB) was collected in 40 μg/mL corn trypsin inhibitor (CTI), 100 μM D-Phe-Pro-Arg-CMK (PPACK), or 50 mM ethylenediaminetetraacetic acid (EDTA) from healthy donors who self-reported to be free of alcohol and medication for at least 48 hr prior to phlebotomy. All donors consented under IRB approval (Univ. Penn.) Platelets were labeled with anti-human CD41 antibody, neutrophils were labeled with anti-human CD11a antibody, and DNA was labeled with Sytox-green (or Hoechst 33342 when indicated).

Microfluidic assay

For coating collagen or collagen/lipidated tissue factor (TF), a single 1000-μm wide channel polydimethylsiloxane (PDMS) patterning device was vacuum-sealed to a Sigmacote-treated glass slide, as previously described [27,28]. A total of 5 μL of 0.5 mg/mL collagen solution (or collagen followed by 5 μL infusion of 7 nM TF) was perfused through the channel to create a prothrombotic coating on the glass. Similarly, 5 μL of 100 μg/ml P-selectin can be used to generate a surface that allows neutrophil adhesion. The patterning device was replaced by an 8-channel PDMS device with each channel (60-μm high x 250-μm wide) positioned perpendicular to the patterned collagen (Fig. S1). Thrombi were formed under pressure-relief mode [27] for an initial wall shear rate of 100 or 1000 s^{-1} at a constant withdrawal flowrate of 1 μL/min or 10 μL/min per channel, respectively. In the pressure-relief mode, four alternating channels were loaded with EDTA-treated WB to abolish all clotting. As thrombi grew in the other four matched channels perfused with FXIIa-inhibited WB (with CTI) or thrombin-inhibited WB (with PPACK), blood flow was diverted to the EDTA-treated WB channels. Additional imaging conditions and hemodynamic information are provided in the Supplement.

Simulation of interstitial flow within platelet clots containing neutrophils (no fibrin)

The Lattice Boltzmann method was used to solve the interstitial velocity field of the Darcy flow around the neutrophil and through the porous gaps formed between platelets of the fully occluding clot. A coarse grained membrane model was used to simulate flow-induced neutrophil deformation and stress. The immersed boundary method (IBM) was used to solve the coupling between the neutrophil deformation and the effective interstitial fluid flow [29,30] (See Supplemental Methods). The computational flow simulation used a subvolume of the thrombosed microfluidic channel corresponding to an *xy*-plane of 40 μm x 40 μm and length of 80-μm along the *z*-axis in the direction of flow. The clot medium was created by random positional insertion of each platelet (either 2 or 3 μm in diameter, picked randomly prior to each insertion event). The resulting porosity of the clot medium was 0.38. The

platelet clot was treated as solid nodes in the fluid domain. A neutrophil was modeled as a coarse-grained membrane that resisted stretching and bending with an area expansion modulus of 40 pN/μm [31,32] and bending stiffness of 1.5×10^{-18} *J* (about 374 k_BT) [33]. The effective neutrophil volume was kept constant (12 μm initial diameter, 452 μm^2, 905 μm^3) and discretized with 10,242 surface nodes and 20,480 triangular elements. A constant pressure gradient (ΔP/L = 70 mmHg/mm-clot) was maintained between the inlet and outlet. A small crevice in the platelet media was implemented to allow the neutrophil to enter the depth of the clot, as observed experimentally. The flow rate decreased as the neutrophil entered the gap formed in the clot media, with an average interstitial flow rate ($\bar{v}A$ = 64 μm/s × 1600 μm^2 at t = 4.8 ms). For a clot with platelet porosity of 0.38, the resulting permeability of the platelet clot was $6.7 \times 10^{-11} cm^2$, consistent with numerous measurements [34].

Results

NETosis is triggered by arterial hemodynamic forces within sterile thrombotic occlusions

For each pair of microchannels perfused at either 2 or 20 μL/min (Fig. 1A–B) to achieve an initial wall shear rate of 100 or 1000 s^{-1}, respectively, one channel allowed active clotting to proceed to occlusion and the other matched channel remained fully open during perfusion with EDTA-treated whole blood. For platelet deposition (no thrombin present with PPACK WB) at an initial wall shear rate of 100 s^{-1} (Fig. 1A), platelets continually accumulated over the course of the 30 min experiment with a slow accumulation of neutrophils (~30 neutrophils along the 1-mm long clot) between 15 and 30 min (Fig. 1C,D) and no detection of NETs (Fig. 1E,F). In contrast, at an initial arterial wall shear rate of 1000 s^{-1}, both platelets and neutrophils continually accumulated (Fig. 1C–D), with a marked generation of NETs between 5 and 30 min (Fig. 1E,G). NETs were detected predominately at the distal end of the occlusive clots formed at arterial conditions as well as interstitial locations where neutrophils became trapped. At occlusion for the arterial pressure-relief condition, a pressure drop per unit length of 163 mm-Hg/mm-clot existed to drive a Darcy flow through the clot, as determined using measurements with pressure sensors (Fig. S2).

The relative lack of neutrophils at the venous condition in Fig. 1 may influence the relative lack of NETs in the clot compared to the arterial condition. To study the effect of hemodynamics on NETosis at a similar neutrophil density, a perfusion shift-up experiment was conducted where flow was increased acutely at 15 min from 2 to 20 μL/min per paired channels (Fig. 2A–C). This shift-up increases the ΔP/L across the occluding clot. NETs were detected within 2 min after perfusion shift-up (Fig. 2C). Under conditions where neutrophil density in the clots were similar (Fig. 2B), NETosis was strongly induced immediately after shift-up to the arterial condition, but remained absent at the venous condition without flow shift-up (Fig. 2D vs. Fig. 2E). Thus, a strong temporal coupling of high hemodynamic forces and NETosis was observed with the rapid onset of NETosis with perfusion shift-up at 15 min. The NETosis driven by flow shift-up was slowed significantly with perfusion shift-down and then began once again with a second event of perfusion shift-up (Fig. 3A–C). To further demonstrate this strong and rapid coupling under full thrombotic conditions (TF present), an increase of perfusion at either 12 or 18 min also resulted in NETosis within 2

minutes of shift-up (Fig. 3D–F). This fully demonstrated how rapidly responsive NETosis was to high hemodynamic forces. Shift-up to 500 s^{-1} (10 μL/min per paired channels) also induced NETosis, while shift-up to 250 s^{-1} (5 μL/min per paired channels) was insufficient to generate a large enough ΔP/L to drive shear-induced NETs (Fig. S3). In a hemodynamic context of 100 s^{-1} initial shear rate that was not sufficient to drive NETosis (ΔP/L = 19 mm-Hg/mm-clot), the addition of *E. coli* to the blood was sufficient to induce NETs within an occlusive clot. The appearance of NETs due to *E. coli* (Fig. S10) was slower and less extensive than that observed for conditions of high shear induced NETosis within sterile occlusive thrombi.

With no thrombin or fibrin production, continuous arterial perfusion resulted in >150-fold increase in NET production relative to the venous condition (Fig. 4A). NETosis also occurred at arterial flow conditions or in the perfusion shift-up experiment (Fig. S4) when thrombin and fibrin were allowed to form during sterile thrombosis. Using CTI-treated whole blood perfused over collagen/tissue factor, a full thrombotic response involving platelet, thrombin, and fibrin polymerization occurred (Fig. 4C–D). With thrombin and fibrin generation, the arterial flow condition drove NET generation to a level that was >80-fold greater than that of the venous condition. Similarly, the perfusion shift-up at 15 min resulted in 52-fold and 90-fold increase in NETs (after 15 min of high flow), relative to no shift-up, in the absence (Fig. 4B) or presence of thrombin/fibrin (Fig. 4D), respectively. Neither thrombin nor fibrin was required for shear-induced NETosis. Additionally, neither thrombin nor fibrin blocked shear-induced NETosis.

For constant flow rate through an 8-channel device lacking the EDTA-WB diversion channels, the flow becomes highly pathological as the growing clot continually narrows the channel lumen. This experimental condition is different from in vivo hemodynamics since vessels do not thrombose at constant flow rate. Under these laboratory microfluidic conditions of clotting at constant flow rate, the syringe pump always is stronger than a clot: the wall shear stress on the clot surface can become quite large (>10^4 dyne/cm^2 at > 80 % occlusion) as will the continually increasing pressure drop on the occlusive clot that sustains an interstitial flowrate set by the infusion pump. In this laboratory configuration of constant flow rate, the superficial flowrate (1 μL/min per channel of cross sectional area of 250 μm x 60 μm) remains precisely well defined by the syringe pump. Under these constant flow conditions, NETosis can also be easily observed (Fig. S5, Video S2) at the constant superficial velocity of $\bar{v}$ = 1.1 mm/sec moving through the occlusive clot (prior to the eventual clot embolism in this constant flow assay).

Shear-induced NETs were not blocked by inhibitors of cyclooxygenase, PSGL-1, CD18, HMGB1, RAGE, ATP/ADP, PAD4, or PI3K

Shear-induced NETs were consistently observed in the distal region of occlusive clots. The NETs were immunopositive for citrullinated histone H3 (CitH3) and were rapidly degraded by DNase, confirming that Sytox-green detects NETs under the microfluidic flow conditions of coagulation (Fig. 5). Interestingly, not all of the released DNA was immunopositive for CitH3 (Fig. 5F) indicating some heterogeneity in the mechanism of NET release. We further tested a number of inhibitors for possible antagonism of shear-induced NETs (Fig. 5J).

Consistent with the observed physical entrapment of neutrophils in the clotted structures, the accumulation of neutrophils and the subsequent release of NETs at arterial conditions was not blocked by anti-PSGL-1 and anti-CD18 despite a delay in neutrophil recruitment (Fig. S6). When combining CD11a/CD11b and CD18 antibodies (Fig. S8 A–C), neutrophils still accumulated, consistent with a physical entrapment mechanism within the platelet mass, and SINs were still detected. Despite the abundance of platelets in the clot structures, inhibitors against platelet mediators had little effect on shear-induced NETs. In the presence of thrombin, cyclooxygenase blockade by aspirin did not affect platelet/neutrophil deposition or NET release. When TF was absent on the collagen surface (Fig. S7), aspirin caused an expected delay and reduction in platelet accumulation under flow [35], which consequently delayed the occlusion time and delayed neutrophil accumulation. At the time of flow shift-up, platelets rapidly accumulated in the presence of ASA and neutrophil accumulation then progressed along with concomitant shear-induced NETosis when the platelet deposits became occlusive. The recombinant protein reBox A that blocks subdomain of HMGB1 [3,4] had no effect on the formation of NETs (Figs 5J, S7). Blocking antibodies against HMGB1 or RAGE had no effect on the extracellular DNA signal. Inhibiting PAD4 with Cl-amidine [36] did not reduce NET generation (Figs 5J, S7). In the absence of thrombin/fibrin generation (Fig. S8 D, F–H), platelet deposition was significantly reduced, as expected, by the PI3K inhibitor Wortmannin and no neutrophil recruitment occurred. Without neutrophils, no DNA release was detected. In contrast, when thrombin generation and fibrin polymerization were triggered with TF (Fig. S8 E, I–K), platelets accumulated even in the presence of Wortmannin, neutrophil were captured, and shear induced NETosis was detected. Under fully thrombotic conditions driven by surface TF where Wortmannin's effect on platelets was overcome, the exposure of neutrophils to PI3K inhibition did not block shear-induced NETosis.

To evaluate if shear induced platelet activation (SIPA) and consequent platelet secretion is driving shear induced NETosis, we conducted 3 separate experiments (Fig. 6) that all demonstrate a lack of any role for SIPA releasate driving shear induced NETosis: (1) high dose addition of two major platelet secretagogues (convulxin+SFLLRN) failed to drive NETosis at low shear; (2) high dose apyrase to target platelet secreted ATP/ADP (the major mediators of SIPA) [37,38] had no effect on shear induced NETosis; and (3) the effluent from an occlusive clot displaying shear induced NETosis was directly contacted with a distal monolayer of P-selectin adherent neutrophils which failed to display any NETosis. While apyrase is the classic approach to block SIPA via ADP release in closed systems (cone-and-plate viscometry of PRP), apyrase is less effective in dense, but non-occlusive wall attached platelet deposits that lack significant intrathrombus permeation [28,39]. In contrast, the pressure-driven permeation of apyrase and ADP is substantially greater for fully occlusive thrombi compared to non-occlusive thrombi.

Simulation of Darcy flow through occlusive clots containing deformable neutrophils

A numerical simulation of pressure-driven Darcy flow through a platelet occlusion was used to calculate the hydrodynamic forces on a deformable neutrophil becoming entrapped in the deposit. In Fig. 7, the calculated local instantaneous velocity in the porous media was non-uniform. The fluid shear rate and shear stress (Fig. 7E–F) near the protruding tip of the

neutrophil could reach as high as 5000 s^{-1} and 15 pa (= 150 dyne/cm^2). Interestingly, the lysis threshold for neutrophils in bulk shear flow in a cone-and-plate viscometer has been measured to be ~15 Pa. Large membrane stresses (>50 Pa) were calculated at the leading edge of the neutrophil as it deformed under hemodynamic loading (Fig. 7D).

Discussion

Shear-induced NETosis was independent of the coagulation processes of thrombin generation and fibrin formation. Clot entrapped neutrophils were clearly in close proximity to activated and dense platelet deposits, however the generation of NETs was largely controlled temporally by the onset of high hemodynamic forces, consistent with the lack of effect of HMGB1/RAGE and PAD4 inhibitors. Similarly, inhibitors of platelet-neutrophil adhesion did not prevent shear-induced NETosis. In the assay, neutrophils were observed to haltingly translocate through crevices and canaliculi of the occlusive thrombi (Video S1), distinct from classical rolling on inflamed endothelium.

In order to observe neutrophil locations prior to NETosis, we conducted the flow shift-up experiment at 20X magnification with a 10 sec time interval after the 13 min time point. In Fig. S9 B–C, the highlighted neutrophils showed up before flow shift-up, stayed inside the clot, and released DNA. The NET releasing neutrophil in Fig. S9 A arrived at the spot after flow shift-up without DNA signal, became trapped in the clot, and then released DNA. Therefore neutrophils entrapped under venous shear were capable of releasing NETs when they were exposed to an elevated pressure drop across the clot. The physical entrapment of neutrophils could occur both before and after flow shift-up and neutrophils may also translocate through the thrombus after shift-up to deliver neutrophils to entrapped positions that then facilitate shear-induced NETosis. Since neutrophils undergoing shear-induced NETosis were already entrapped and not moving with high velocity or experiencing high collision rates or rolling, the shear stress, not the shear rate, of the permeating flow would be the most likely driver of SINs (see Supplemental Discussion).

In static incubation assays utilizing platelet activating factor, ionomycin, or phorbol ester and lasting several hours, platelet P-selectin was found to promote NETosis [40]. Other studies using both static and flow assays, however, found platelet P-selectin was not required for NETosis driven by LPS for 60 min [41] or driven by activated platelets releasing HMGB1 [3]. During microfluidic clotting, we observed that PSGL-1 and CD18 blocking antibodies used together impaired the platelet-neutrophil interactions as demonstrated by the modest delay in neutrophil accumulation, however, physically entrapped neutrophils still released extracellular DNA at the onset of high shear stress. Also, ASA has been reported to reduce NETosis during TRALI [17] or experimental peritonitis [42]. However, neutrophil response to platelet derived thromboxane is not well defined (absent the thromboxane receptor) and ASA may have direct effects on neutrophils via COX2-dependent PGE_2 production [43] that may inhibit NETosis to some extent [44]. We found that thromboxane antagonism with ASA reduced platelet accumulation and subsequent occlusion, but ultimately did not prevent shear-induced NETs. In addition, we conclude that shear-induced NET production appears to be a process that does not require paracrine signals from shear induced platelet activation (SIPA) during sterile thrombosis.

In these microfluidic experiments, the essential hemodynamic condition to drive SINs was a ΔP/L of ~ 87 to 163 mm-Hg/mm-clot (Fig. S2) across the occlusive clot. In humans, a 0.1 mm-long occlusive clot within an arteriole would experience ΔP/L ~ (70 – 30 mm-Hg)/0.1 mm-clot = 400 mm-Hg/mm-clot as the blood distal of the clot depressurizes to the capillary inlet pressure. We conclude that sterile arteriole occlusions during DIC experience hemodynamics forces sufficient to drive shear-induced NETs. Interestingly, patients with sepsis display elevated plasma level of NETs if they also experience DIC [14]. Our results indicate that arteriole thrombosis can generate NETs as a result of intrathrombus hemodynamic shear forces. Additionally, we hypothesize that thrombotic occlusions between the arterial and venous system (AV fistula) may be potentially susceptible to large intrathrombic forces that render the occlusion especially prone to shear induced NETosis.

During hemostasis, sterile hemostatic clots within a punctured arteriole or artery wall connect the arterial blood compartment pressure (70 to 120 mm-Hg) to an interstitial pressure compartment (5 - 10 mm-Hg) or to the atmosphere (0 mm-Hg). Such hemostatic clots experience a ΔP/L ranging from 60 to 1200 mm-Hg/mm-clot for clots that are 0.1 to 1 mm in dimension between compartments. An occlusive hemostatic clot at the end of a fully severed arteriole would experience a similar range of ΔP/L, depending on length. In the context of hemostatic clots, shear-induced NETs might represent an anti-microbial barrier on the outer surface of the clot facing contamination during wounding. In the context of internal intrathoracic injury, the possibility of subatmospheric interstitial pressures (−10 mm-Hg) via diaphragm mechanics would further increase pressure drops across the hemostatic clots sealing injured vessels.

NETs have been recently identified within coronary thrombi [13]. Mangold et al. reported that coronary thrombi contained significantly more NETs than venous thrombi, and they observed no NETs in clot formed in vitro under static conditions. While other factors such as cholesterol crystals could also play a role, it is possible that shear stress may contribute to the higher NET level found in coronary thrombi. A small occlusive thrombus (L = 1 mm in length) within a stenosed artery would experience peak ΔP/L ~ 100 mm-Hg/mm-clot, sufficient to drive shear-induced NETs, assuming distal capillary flow stops and depressurizes to the venous pressure (10 mm-Hg). In contrast, partial coronary occlusions may experience little interstitial permeation, but would experience pathologically high wall shear stresses on their outer boundary exposed to flow, a driving force for von Willebrand Factor unfolding [45]. Furthermore, the rapid shear-induced NET release implies the possibility that hemodynamic forces may become an important mediator of neutrophil extracellular DNA as thrombosis approaches the instant of full vessel occlusion. Because hemodynamic forces are driven by ΔP/L across a clot, extreme hypertension might exacerbate shear-induced NETosis following sterile thrombotic occlusion.

Venous clots that are many centimeters in length likely have minimal interstitial flow to drive shear-induced NETosis. While DVT occurs in the setting of low flow or stasis and can present NETs [12], the final DVT in patients results in arterial pressures upstream of the clot (and consequent extreme venous dilation, the radiological signature of DVT) and venous pressures downstream of the clot. A pressure drop of ~100 mm-Hg over an initiating venous clot length of 1 mm might create substantial interstitial shear stress due to permeation.

However, the size of the venous valve pocket would suggest that an occluding venous clot would have to be several millimeters in length with a pressure drop less than what was found necessary to drive shear-induced NETs.

The flow upshift experiment resulted in rapid NETosis within 2 min. In contrast, pathogens have been shown to induce vital NETosis within an hour [46] and incubation of neutrophils in vitro with 50 nM PMA or 20 ng/mL TNFα requires 180 min for suicidal NET generation [42]. A variety of pore-forming cytolytic toxins have also been reported to induce NET generation [47,48]. This suggests shear-induced formation of membrane pores may be sufficient to trigger NETosis. Indeed, Malachowa et al [48] reported that neutrophils exposed to electroporation release diffuse DNA that resembles PMA-induced NET structures. While electroporation is not physiological, our results demonstrate that fluid shear stress and large membrane stresses may render neutrophils vulnerable to membrane disruption and NETosis. By simulation of flow in dense clots, we calculate that hemodynamic forces on neutrophils in clots can substantially exceed the shear stress lysis threshold of 15 Pa needed to drive neutrophil lysis in a cone-and-plate viscometer.

To our knowledge, this is the first report of hemodynamic forces driving rapid NETosis within sterile occlusive thrombi. NETs generated in response to pathophysiological hemodynamic stress might have thrombotic or inflammatory properties similar to NETs triggered by other stimuli. The role of shear-induced NETs in the context of sickle cell crisis and other schistocyte-positive microangiopathies [49] remains to be explored.

Supplementary Material

Refer to Web version on PubMed Central for supplementary material.

Acknowledgments

This study was supported by National Institutes of Health grants U01-HL-131053 and R01-HL-103419 to S. L. Diamond.

References

1. Brinkmann V, Reichard U, Goosmann C, Fauler B, Uhlemann Y, Weiss DS, Weinrauch Y, Zychlinsky A. Neutrophil extracellular traps kill bacteria. Science. 2004; 303:1532–5. [PubMed: 15001782]
2. Urban CF, Reichard U, Brinkmann V, Zychlinsky A. Neutrophil extracellular traps capture and kill Candida albicans yeast and hyphal forms. Cell Microbiol. 2006; 8:668–76. [PubMed: 16548892]
3. Maugeri N, Campana L, Gavina M, Covino C, De Metrio M, Panciroli C, Maiuri L, Maseri A, D'Angelo A, Bianchi ME, Rovere-Querini P, Manfredi AA. Activated platelets present high mobility group box 1 to neutrophils, inducing autophagy and promoting the extrusion of neutrophil extracellular traps. J Thromb Haemost. 2014; 12:2074–88. [PubMed: 25163512]
4. Stark K, Philippi V, Stockhausen S, Busse J, Antonelli A, Miller M, Schubert I, Hoseinpour P, Chandraratne S, Von M-L, Uhl B, Gaertner F, Lorenz M, Agresti A, Coletti R, Antoine DJ, Heermann R, Jung K, Reese S, Laitinen I, et al. Disulfide HMGB1 derived from platelets coordinates venous thrombosis in mice. Blood. 2016; 128:2435–49. [PubMed: 27574188]
5. Kessenbrock K, Krumbholz M, Schönermarck U, Back W, Gross WL, Werb Z, Gröne H-J, Brinkmann V, Jenne DE. Netting neutrophils in autoimmune small-vessel vasculitis. Nat Med. 2009; 15:623–5. [PubMed: 19448636]

6. Noubouossie DF, Whelihan MF, Yu Y-B, Sparkenbaugh E, Pawlinski R, Monroe DM, Key NS. In vitro activation of coagulation by human neutrophil DNA and histone proteins but not neutrophil extracellular traps. Blood. 2017; 129:1021–9. [PubMed: 27919911]
7. Fuchs TA, Brill A, Duerschmied D, Schatzberg D, Monestier M, Myers DD, Wrobleski SK, Wakefield TW, Hartwig JH, Wagner DD. Extracellular DNA traps promote thrombosis. Proc Natl Acad Sci U S A. 2010; 107:15880–5. [PubMed: 20798043]
8. Gould TJ, Vu TT, Swystun LL, Dwivedi DJ, Mai SHC, Weitz JI, Liaw PC. Neutrophil extracellular traps promote thrombin generation through platelet-dependent and platelet-independent mechanisms. Arterioscler Thromb Vasc Biol. 2014; 34:1977–84. [PubMed: 25012129]
9. Massberg, S., Grahl, L., von Bruehl, M-L., Manukyan, D., Pfeiler, S., Goosmann, C., Brinkmann, V., Lorenz, M., Bidzhekov, K., Khandagale, AB., Konrad, I., Kennerknecht, E., Reges, K., Holdenrieder, S., Braun, S., Reinhardt, C., Spannagl, M., Preissner, KT., Engelmann, B. Nat Med. Vol. 16. Nature Publishing Group; 2010. Reciprocal coupling of coagulation and innate immunity via neutrophil serine proteases; p. 887-96.
10. Kaplan MJ, Radic M. Neutrophil extracelullar traps (NETs):Double-edged swords of innate immunity 1. J Immunol. 2012; 189:2689–95. [PubMed: 22956760]
11. Clark SR, Ma AC, Tavener SA, McDonald B, Goodarzi Z, Kelly MM, Patel KD, Chakrabarti S, McAvoy E, Sinclair GD, Keys EM, Allen-Vercoe E, Devinney R, Doig CJ, Green FHY, Kubes P. Platelet TLR4 activates neutrophil extracellular traps to ensnare bacteria in septic blood. Nat Med. 2007; 13:463–9. [PubMed: 17384648]
12. Von Brühl M-L, Stark K, Steinhart A, Chandraratne S, Konrad I, Lorenz M, Khandoga A, Tirniceriu A, Coletti R, Köllnberger M, Byrne RA, Laitinen I, Walch A, Brill A, Pfeiler S, Manukyan D, Braun S, Lange P, Riegger J, Ware J, et al. Monocytes, neutrophils, and platelets cooperate to initiate and propagate venous thrombosis in mice in vivo. J Exp Med. 2012; 209:819–35. [PubMed: 22451716]
13. Mangold A, Alias S, Scherz T, Hofbauer T, Jakowitsch J, Panzenböck A, Simon D, Laimer D, Bangert C, Kammerlander A, Mascherbauer J, Winter MP, Distelmaier K, Adlbrecht C, Preissner KT, Lang IM. Coronary neutrophil extracellular trap burden and deoxyribonuclease activity in ST-elevation acute coronary syndrome are predictors of ST-segment resolution and infarct size. Circ Res. 2015; 116:1182–92. [PubMed: 25547404]
14. Delabranche X, Stiel L, Severac F, Galoisy A-C, Mauvieux L, Zobairi F, Lavigne T, Toti F, Anglès-Cano E, Meziani F, Boisramé-Helms J. Evidence of Netosis in Septic Shock-Induced Disseminated Intravascular Coagulation. SHOCK. 2017; 47:313–7. [PubMed: 27488091]
15. Margraf S, Lögters T, Reipen J, Altrichter J, Scholz M, Windolf J. Neutrophil-derived circulating free DNA (cf-DNA/NETs): a potential prognostic marker for posttraumatic development of inflammatory second hit and sepsis. Shock. 2008; 30:352–8. [PubMed: 18317404]
16. Liu F-C, Chuang Y-H, Tsai Y-F, Yu H-P. Role of neutrophil extracellular traps following injury. Shock. 2014; 41:491–8. [PubMed: 24837201]
17. Caudrillier A, Kessenbrock K, Gilliss BM, Nguyen JX, Marques MB, Monestier M, Toy P, Werb Z, Looney MR. Platelets induce neutrophil extracellular traps in transfusion-related acute lung injury. J Clin Invest. 2012; 122:2661–71. [PubMed: 22684106]
18. Kaplan, ZS., Zarpellon, A., Alwis, I., Yuan, Y., McFadyen, J., Ghasemzadeh, M., Schoenwaelder, SM., Ruggeri, ZM., Jackson, SP. Nat Commun. Vol. 6. Nature Publishing Group; 2015. Thrombin-dependent intravascular leukocyte trafficking regulated by fibrin and the platelet receptors GPIb and PAR4; p. 7835
19. Konstantopoulos K, Neelamegham S, Burns AR, Hentzen E, Kansas GS, Snapp KR, Berg EL, David Hellums J, Wayne Smith C, McIntire LV, Simon SI. Venous Levels of Shear Support Neutrophil-Platelet Adhesion and Neutrophil Aggregation in Blood via P-Selectin and β2-Integrin. Circulation. 1998; 98:873–82. [PubMed: 9738642]
20. Jorch SK, Kubes P. An emerging role for neutrophil extracellular traps in noninfectious disease. Nat Med. 2017; 23:279–87. [PubMed: 28267716]
21. Wang Y, Li M, Stadler S, Correll S, Li P, Wang D, Hayama R, Leonelli L, Han H, Grigoryev SA, Allis CD, Coonrod SA. Histone hypercitrullination mediates chromatin decondensation and neutrophil extracellular trap formation. J Cell Biol. 2009; 184:205–13. [PubMed: 19153223]

22. Rochael NC, Guimarães-Costa AB, Nascimento CMT, DeSouza-Vieira TS, Oliveira MP, Garcia Souza LF, Oliveira MF, Saraiva EM. Classical ROS-dependent and early/rapid ROS-independent release of Neutrophil Extracellular Traps triggered by Leishmania parasites. Sci Rep. 2015; 5:18302. [PubMed: 26673780]

23. Lewis HD, Liddle J, Coote JE, Atkinson SJ, Barker MD, Bax BD, Bicker KL, Bingham RP, Campbell M, Hua Chen Y, Chung C, Craggs PD, Davis RP, Eberhard D, Joberty G, Lind KE, Locke K, Maller C, Martinod K, Patten C, et al. Inhibition of PAD4 activity is sufficient to disrupt mouse and human NET formation. Nat Chem Biol. 2015; 11:189–91. [PubMed: 25622091]

24. Moussavi-Harami SF, Mladinich KM, Sackmann EK, Shelef MA, Starnes TW, Guckenberger DJ, Huttenlocher A, Beebe DJ. Microfluidic device for simultaneous analysis of neutrophil extracellular traps and production of reactive oxygen species. Integr Biol. 2016; 8:243–52.

25. Boneschansker, L., Inoue, Y., Oklu, R., Irimia, D. Integr Biol. Vol. 8. Royal Society of Chemistry; 2016. Capillary plexuses are vulnerable to neutrophil extracellular traps; p. 149-55.

26. Brass LF, Diamond SL. Transport physics and biorheology in the setting of hemostasis and thrombosis. J Thromb Haemost. 2016; 14:906–17. [PubMed: 26848552]

27. Colace TV, Muthard RW, Diamond SL. Thrombus Growth and Embolism on Tissue Factor-Bearing Collagen Surfaces Under Flow Role of Thrombin With and Without Fibrin. Arterioscler Thromb Vasc Biol. 2012; 32:1466–76. [PubMed: 22516070]

28. Maloney SF, Brass LF, Diamond SL. P2Y12 or P2Y1 inhibitors reduce platelet deposition in a microfluidic model of thrombosis while apyrase lacks efficacy under flow conditions. Integr Biol (Camb). 2010; 2:183–92. [PubMed: 20473398]

29. Peskin CS. The immersed boundary method. Acta Numer. 2002; 11:479–517.

30. Fogelson AL, Guy RD. Immersed-boundary-type models of intravascular platelet aggregation. Comput Methods Appl Mech Eng. 2008; 197:2087–104.

31. Hochmuth RM. Micropipette aspiration of living cells. J Biomech. 2000; 33:15–22. [PubMed: 10609514]

32. Needham D, Hochmuth RM. A sensitive measure of surface stress in the resting neutrophil. Biophys J. 1992; 61:1664–70. [PubMed: 1617145]

33. Zhelev DV, Needham D, Hochmuth RM. Role of the membrane cortex in neutrophil deformation in small pipets. Biophys J. 1994; 67:696–705. [PubMed: 7948682]

34. Wufsus, AR., Macera, NE., Neeves, KB. Biophys J. Vol. 104. Biophysical Society; 2013. The hydraulic permeability of blood clots as a function of fibrin and platelet density; p. 1812-23.

35. Li R, Fries S, Li X, Grosser T, Diamond SL. Microfluidic assay of platelet deposition on collagen by perfusion of whole blood from healthy individuals taking aspirin. Clin Chem. 2013; 59:1195–204. [PubMed: 23592503]

36. Knight JS, Zhao W, Luo W, Subramanian V, O'Dell AA, Yalavarthi S, Hodgin JB, Eitzman DT, Thompson PR, Kaplan MJ. Peptidylarginine deiminase inhibition is immunomodulatory and vasculoprotective in murine lupus. J Clin Invest. 2013; 123:2981–93. [PubMed: 23722903]

37. Moake JL, Turner NA, Stathopoulos NA, Nolasco L, Hellums JD. Shear-induced platelet aggregation can be mediated by vWF released from platelets, as well as by exogenous large or unusually large vWF multimers, requires adenosine diphosphate, and is resistant to aspirin. Blood. 1988; 71:1366–74. [PubMed: 3258770]

38. Oury C, Sticker E, Cornelissen H, De Vos R, Vermylen J, Hoylaerts M. ATP augments von Willebrand factor-dependent shear-induced platelet aggregation through Ca2+-calmodulin and myosin light chain kinase activation. J Biol Chem. 2004; 279:26266–73. [PubMed: 15087444]

39. Tomaiuolo, M., Stalker, TJ., Welsh, JD., Diamond, SL., Sinno, T., Brass, LF. Blood. Vol. 124. American Society of Hematology; 2014. A systems approach to hemostasis: 2. Computational analysis of molecular transport in the thrombus microenvironment; p. 1816-23.

40. Etulain J, Martinod K, Wong SL, Cifuni SM, Schattner M, Wagner DD. P-selectin promotes neutrophil extracellular trap formation in mice. Blood. 2015; 126:242–6. [PubMed: 25979951]

41. Carestia A, Kaufman T, Rivadeneyra L, Landoni VI, Pozner RG, Negrotto S, Paola D, 'atri L, Gómez RM, Schattner M. Mediators and molecular pathways involved in the regulation of neutrophil extracellular trap formation mediated by activated platelets. J Leukoc Biol. 2016; 99:153–62. [PubMed: 26320263]

42. Lapponi MJ, Carestia A, Landoni VI, Rivadeneyra L, Etulain J, Negrotto S, Pozner RG, Schattner M. Regulation of neutrophil extracellular trap formation by anti-inflammatory drugs. J Pharmacol Exp Ther. 2013; 345:430–7. [PubMed: 23536315]

43. St-Ongea M, Flamandb N, Biarca J, Picarda S, Boucharda L, Dussaulta A-A, Laflammea C, Jamesc MJ, Caugheyc GE, Clelandc LG, Borgeata P, Pouliota M. Characterization of prostaglandin E2 generation through the cyclooxygenase (COX)-2 pathway in human neutrophils. Biochim Biophys Acta. 2007; 1771:1235–45. [PubMed: 17643350]

44. Shishikura K, Horiuchi T, Sakata N, Trinh DA, Shirakawa R, Kimura T, Asada Y, Horiuchi H. Prostaglandin E2 inhibits neutrophil extracellular trap formation through production of cyclic AMP. Br J Pharmacol. 2016; 173:319–31. [PubMed: 26505736]

45. Colace TV, Diamond SL. Direct observation of von Willebrand factor elongation and fiber formation on collagen during acute whole blood exposure to pathological flow. Arterioscler Thromb Vasc Biol. 2013; 33:105–13. [PubMed: 23104847]

46. Yipp BG, Petri B, Salina D, Jenne CN, Scott BN, Zbytnuik LD, Pittman K, Asaduzzaman M, Wu K, Meijndert HC, Malawista SE, de Boisfleury Chevance A, Zhang K, Conly J, Kubes P. Infection-induced NETosis is a dynamic process involving neutrophil multitasking in vivo. Nat Med. 2012; 18:1386–93. [PubMed: 22922410]

47. Pilsczek FH, Salina D, Poon KK, Fahey C, Yipp BG, Sibley CD, Robbins SM, Green FH, Surette MG, Sugai M, Bowden MG, Hussain M, Zhang K, Kubes P. A novel mechanism of rapid nuclear neutrophil extracellular trap formation in response to Staphylococcus aureus. J Immunol. 2010; 185:7413–25. [PubMed: 21098229]

48. Malachowa N, Kobayashi SD, Freedman B, Dorward DW, DeLeo FR. Extracellular Traps Promotes Formation of Neutrophil Leukotoxin GH Staphylococcus aureus Staphylococcus aureus Leukotoxin GH Promotes Formation of Neutrophil Extracellular Traps. J Immunol Mater Suppl J Immunol. 2013; 191:6022–9.

49. Jiménez-Alcázar M, Napirei M, Panda R, Köhler EC, Kremer Hovinga JA, Mannherz HG, Peine S, Renné T, Lämmle B, Fuchs TA. Impaired DNase1-mediated degradation of neutrophil extracellular traps is associated with acute thrombotic microangiopathies. J Thromb Haemost. 2015; 13:732–42. [PubMed: 25418346]

Essentials

- Neutrophils extracellular traps (NETs) are generated during thrombosis and sepsis.
- The effect of hemodynamics on NETosis during sterile thrombosis was studied using microfluidics.
- Pressure gradients >70 mmHg/mm-clot across sterile occlusions drive shear-induced NETosis.
- High interstitial hemodynamic forces trigger rapid NET release.

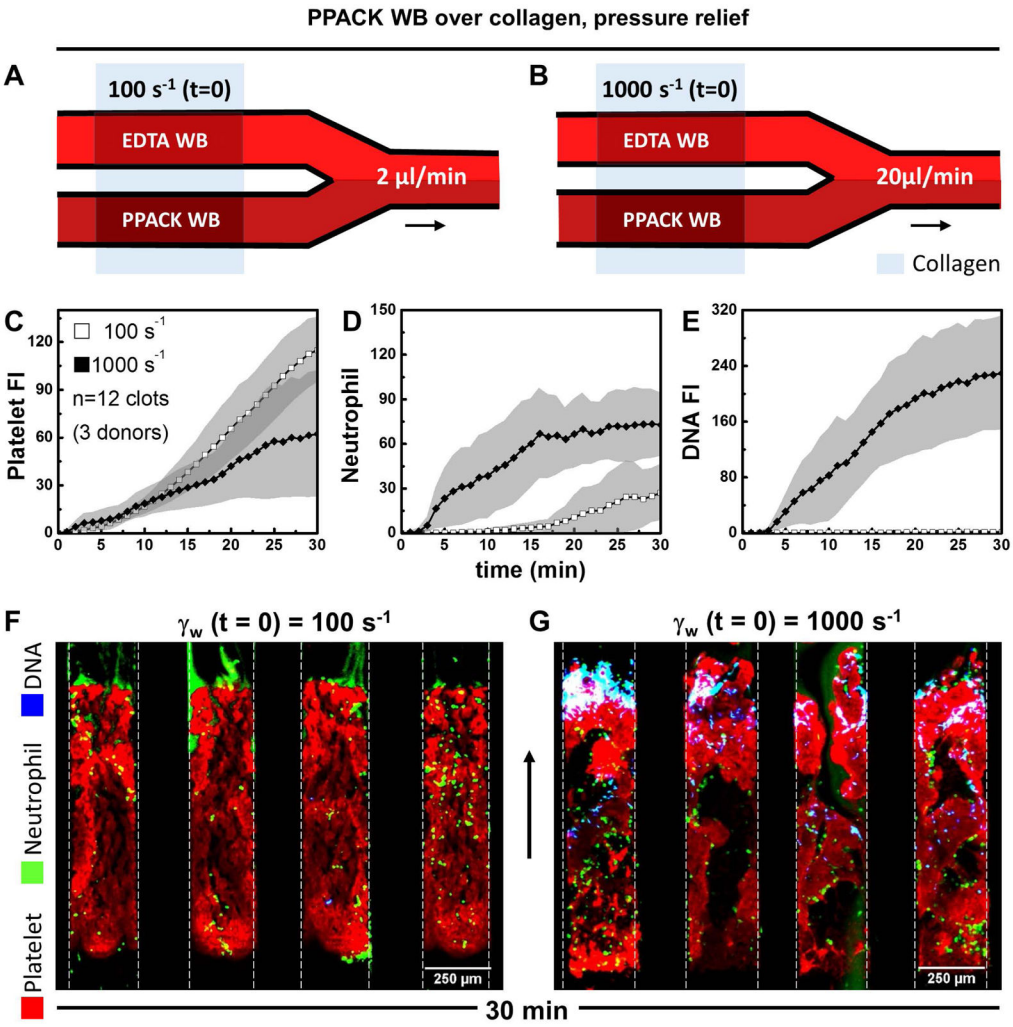

Figure 1.

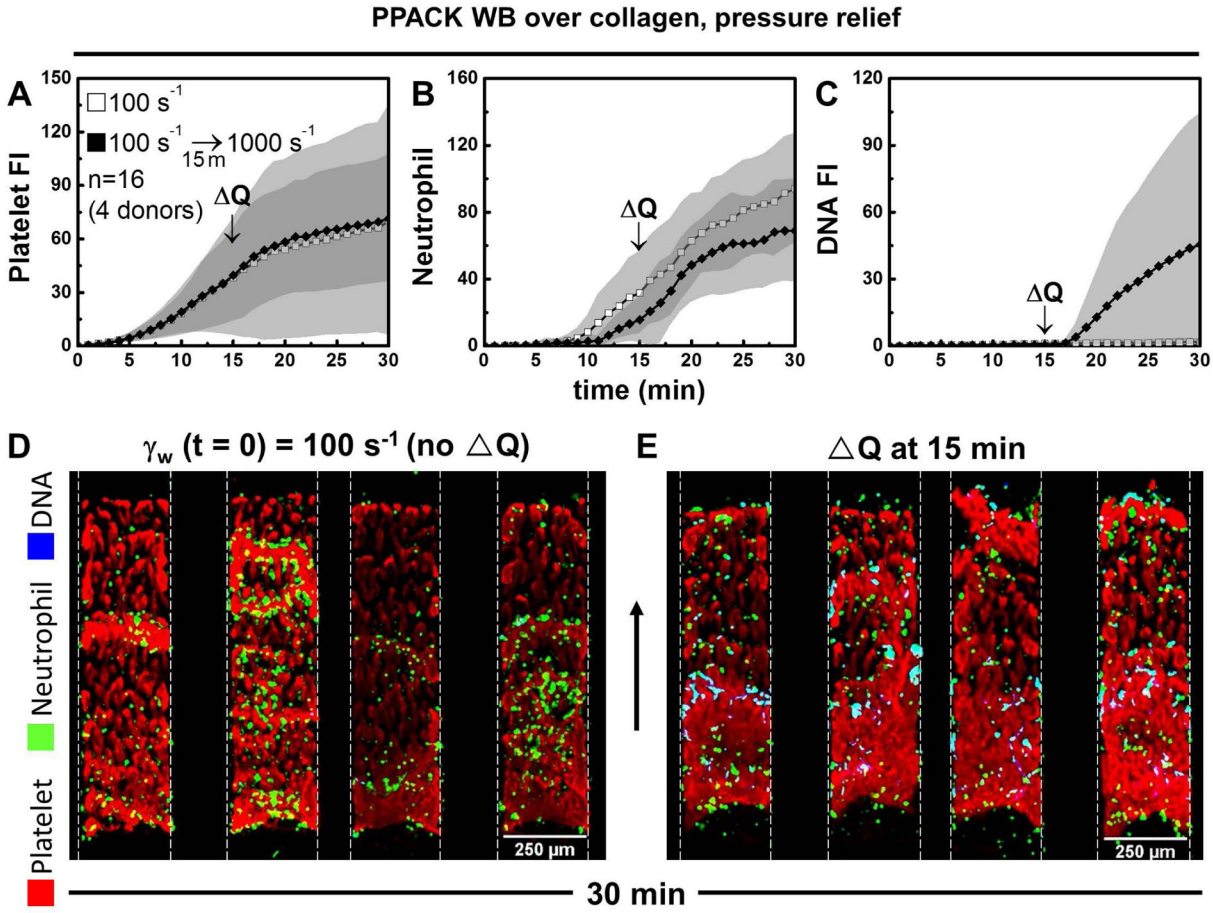

Figure 2.

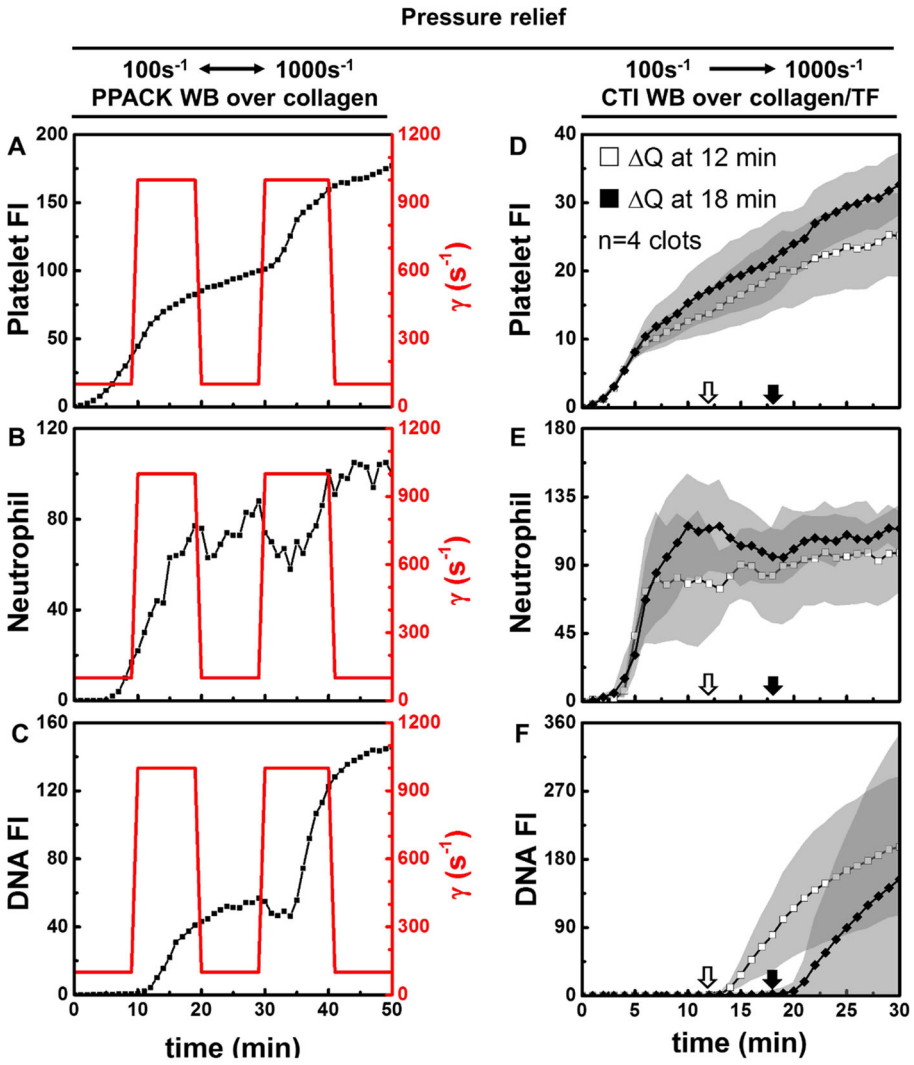

Figure 3.

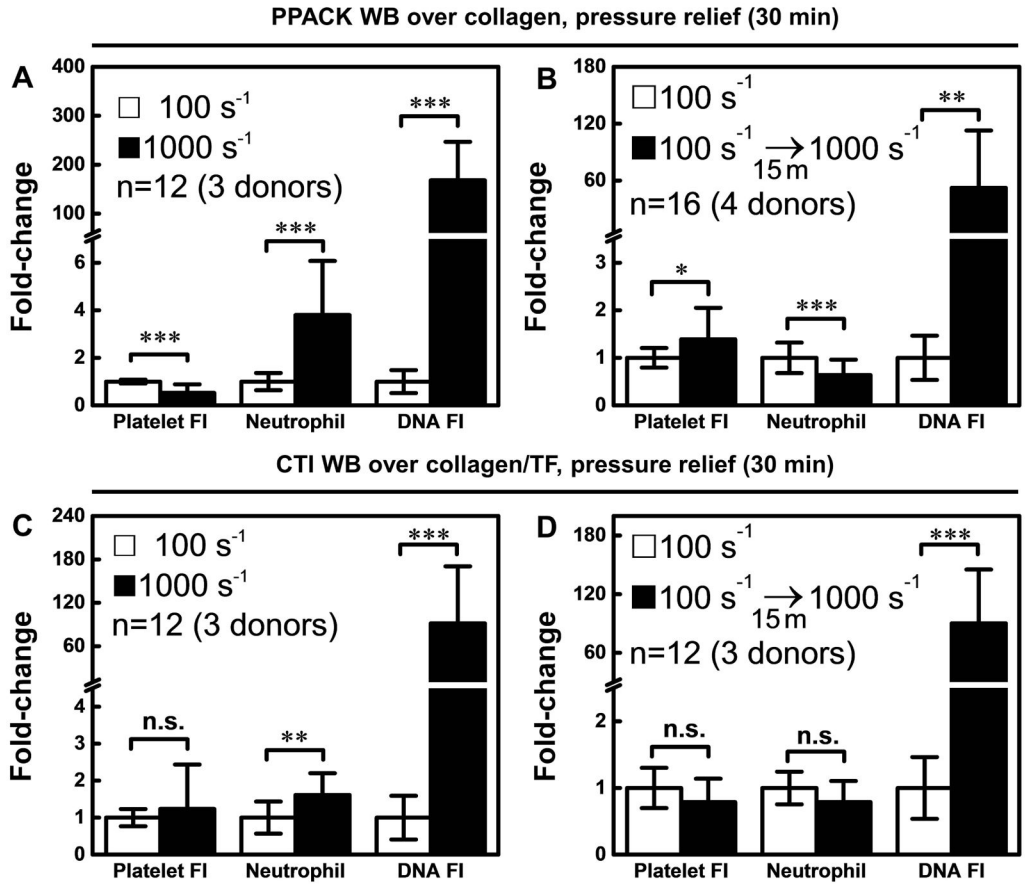

Figure 4.

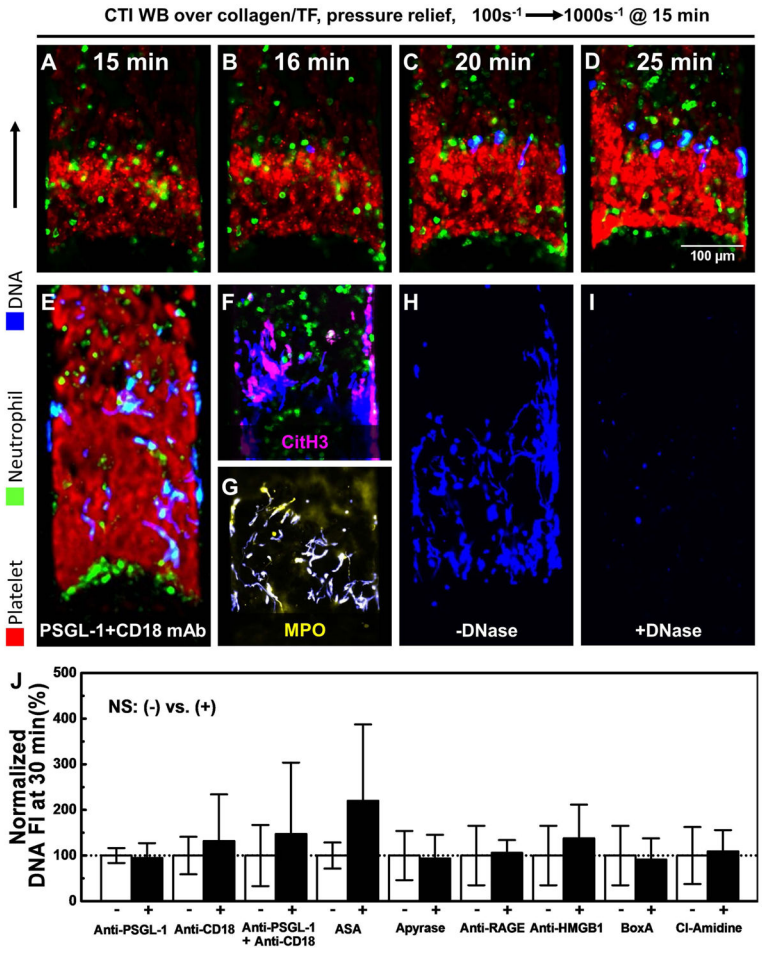

Figure 5.

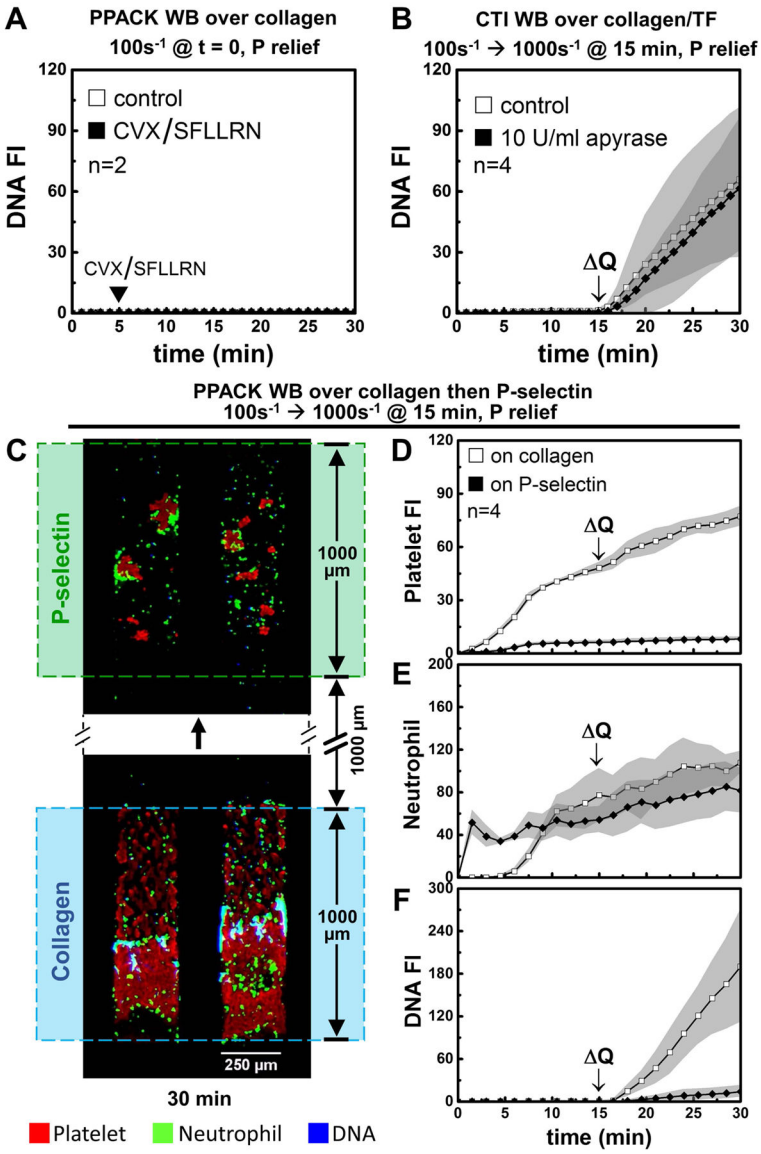

Figure 6.

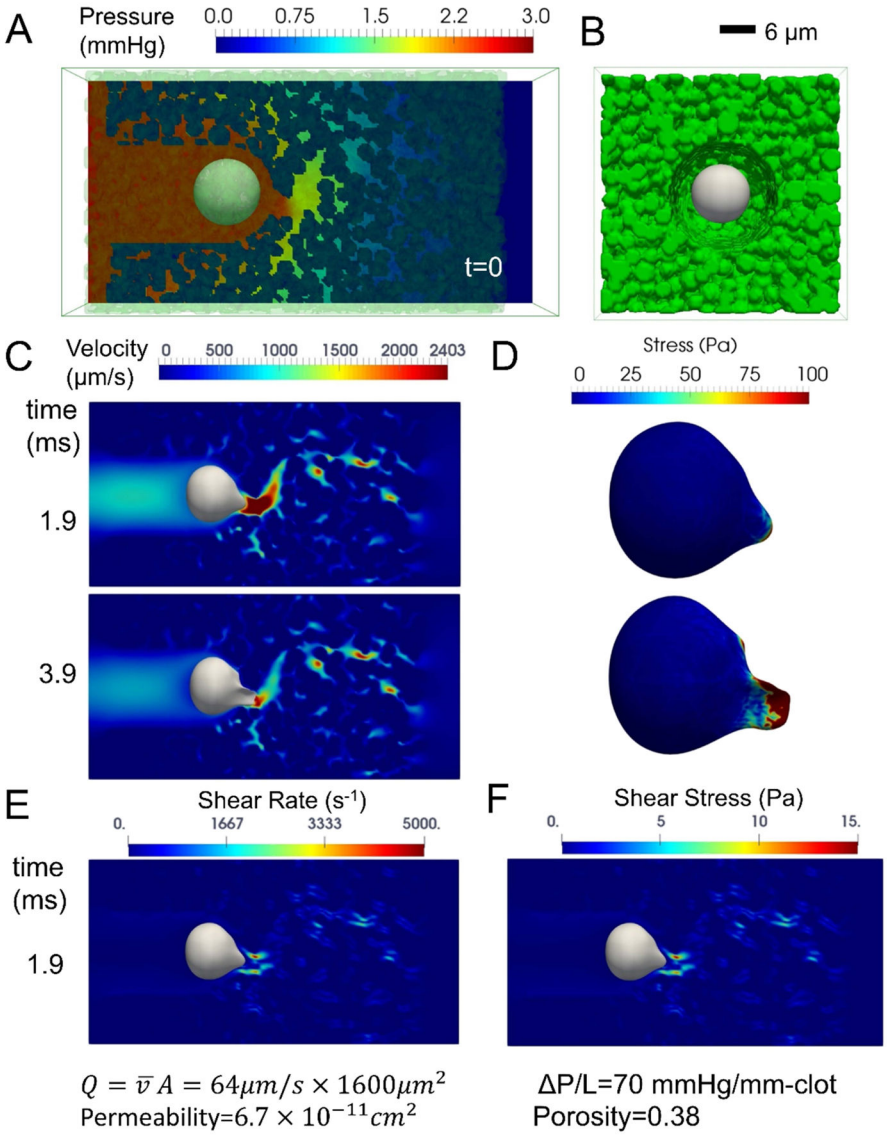

Figure 7.